



# Fabrication and Characterization of ALG Cardiac Patches Enriched with GO: Potential for Angiogenesis of HUVECs

## ARTICLE INFO

### Article Type

Original Research

### Authors

Mahnaz Fathi <sup>1</sup>  
Nafiseh Baheiraei <sup>2\*</sup>  
Saeid Kaviani <sup>1</sup>

1-Department of Hematology, Faculty of Medical Sciences, Tarbiat Modares University, Tehran, Iran

2-Department of Anatomical Sciences, Faculty of Medical Sciences, Tarbiat Modares University, Tehran, Iran

### \*Corresponding authors:

Nafiseh Baheiraei  
Tissue Engineering and Applied Cell Sciences Division, Department of Anatomical Sciences, Faculty of Medical Sciences, Tarbiat Modares University, Tehran, Iran.  
Postal Code: 1411713116.  
Phone: +98 (21) 82884853  
n.baheiraei@modares.ac.ir

## ABSTRACT

**Introduction.** Cardiac infarction is the leading cause of death worldwide. Although conventional treatments, such as medication and various grafts, are unable to restore damaged myocardium effectively, cardiac patch is a promising tissue engineering technique that can stimulate the natural regeneration process of injured tissue via a scaffold with appropriate mechanical properties, biocompatibility, and electrical conductivity.

**Methods.** In this study, the composite scaffolds based on alginate (ALG) were fabricated through freeze-drying and coated with different concentrations of graphene oxide (GO) to make ALG/xGO (x=0.01, 0.05 and 0.1 wt. %) scaffolds. The scaffolds were characterized in terms of morphology, physicochemical structure, tensile strength, electrical conductivity, and cell response and gene expression.

**Results.** The presence of GO provided interconnected pores in the composite scaffolds. Adding GO up to 0.1 wt.% significantly enhanced Young's modulus up to 5.5 MPa and electrical conductivity up to 8.59 S.m<sup>-1</sup> (p≤0.05). Additionally, GO improved the vitality of human umbilical vein endothelial cells (HUVECs) compared to the scaffold without GO. Cell attachment studies on L929 fibroblasts revealed that a 0.05 wt.% GO content can give better sites for cellular nesting due to the suitable size of pores for cell/material interactions.

**Conclusion.** The increase in the amount of GO up to 0.1 wt.% lead to a significant increase in gene expression of VEGFR-2 compared to the other scaffolds and tissue culture plate. The created ALG/0.1GO composite scaffold was found to be suitable for further investigations on cardiac tissue engineering applications.

**Keywords:** angiogenesis, heart patch, alginate, graphene oxide, cardiac tissue engineering

Copyright© 2020, TMU Press. This open-access article is published under the terms of the Creative Commons Attribution-NonCommercial 4.0 International License which permits Share (copy and redistribute the material in any medium or format) and Adapt (remix, transform, and build upon the material) under the Attribution-NonCommercial terms

## INTRODUCTION

Damage to the cardiac muscles is a crucial precursor to heart failure, which is thought to be the leading cause of mortality worldwide [1]. The most common form of cardiovascular disease is myocardial infarction (MI), which is often brought on by "atherosclerosis," a blockage of the coronary arteries, and is followed by the cellular death of millions of cardiomyocytes (CMs) [2]. The poor capacity of CMs for proliferation and regeneration prevents them from replacing the lost cells, which makes it difficult to sustain

cardiac function. [2]. Currently available treatments including medicines and surgical transplant have their own limitations since they are not able to prevent the progression of heart diseases to the last stage and restore the lost cardiac tissue. Employing cell therapy via stem cells presents promising results as a treatment strategy for MI patients. Although cell therapy may prevent ventricular dilation and cardiac dysfunction in patients suffering from MI, some restrictions, such as difficulties in selecting the appropriate cell type for transplantation, mode of

cell delivery, paracrine signaling and homing still exist. Besides, lack of efficient coupling of donor cells with viable host tissues can significantly hinder their electrical communication preventing appropriate engraftment [3, 4].

Cardiac tissue engineering is a promising method for replacing damaged tissue with regenerated tissue that mimics the tissue's natural state. [5]. One of the treatments based on heart tissue engineering, is a 3D polymeric patch placed in the damaged zone with or without cells which can be integrated with its surrounding tissues or replaced with the damaged tissue over time. In fact, the patch acts as an scaffold to deliver the cells into the target tissue and improve the heart's function through providing a mechanical support until the initial stages of healing and regenerations of the diseased tissue [6]. Many types of materials including natural and synthetic polymers have been used to fabricate cardiac patches with different properties. Natural polymers such as collagen [7], gelatin, fibrin [8], fibrinogen [9] and chitosan [10] improve cellular functions such as attachment, proliferation, and differentiation. Tunable degradation and non-toxicity of products resulting from their degradation are other important features of these polymers [11]. Among natural materials, alginate (ALG) has recently attracted the attention for studies due to its biocompatibility, anticoagulant nature, availability, cost-efficiency, desirable gelation ability and the U.S. food and drug administration (FDA) approval [12]. It is reported that using ALG as injectable form for cardiac regeneration of rats can act as an inhibitor for adverse heart regeneration in MI [13]. It is also reported that using composites structure based on ALG hydrogels induced the formation of blood vessels through rapid release of vascular endothelial growth factor (VEGF) and inhibition of myocardial fibrosis [14].

Cardiac muscle is an involuntary electroactive tissue, which forms the main tissue of the heart wall. It is also able to transfer electrical signals and allow the heart to beat. The synchronized response of CMs to electrical signals requires their electromechanical coupling. MI often impairs the cardiac electrical conduction that can severely damage cardiac performance. Therefore, selecting appropriate electroactive

materials to fabricate cardiac patches is of special importance due to the limited ability of poorly conductive patches to contract effectively as a unit. [6, 7, 15, 16]. Different electroactive moieties, such as conductive polymers or their oligomers, carbon nanotubes, carbon nanofibers, gold nanowires, and even naturally derived materials and molecules, such as the melanin pigment, have been widely incorporated within polymeric scaffolds to promote electrical conductivity of cell-seeded scaffolds [4, 18, 19].

In recent times, graphene-based nanomaterials such as graphene oxide (GO) have been widely considered as promising candidates for several biomedical applications, including drug delivery via the nanocarrier approach and tissue engineering due to a wide range of unprecedented properties such as high mechanical stiffness and strength, electrical conductivity, and bioactivity. According to the recent studies, GO has been reported to have good biocompatibility. It can also develop the mechanical properties of scaffolds and improve cellular behaviors including cell adhesion and differentiation in various tissue engineering applications.<sup>36</sup> Tremendous waves of researches have been going on to discover the potential of reduced form of GO (rGO) for MI treatment, as well. It has been reported that the incorporation of rGO flakes, with high electrical activity, into mesenchymal stem cells (MSC) spheroids implanted into the mouse-infarcted myocardium can effectively overexpress angiogenic growth factors and connexin 43 (Cx43) [17]. Using GO as a reinforcement material in cardiac scaffolds enhance the intracellular signaling and cell-ECM interactions [18], while it can reduce inflammation and improve the heart function [4]. It is reported that the presence of GO effectively increases cell viability, electrical conductivity, angiogenesis and expression of the troponin-T and actin-4 [20].

Recently, a series of electroactive cardiac patches have been successfully fabricated by our group, using chemical coating of GO onto the collagen scaffolds followed by reduction of the oxygen containing-groups of GO. Different concentrations of GO were used in order to evaluate its effects on conductivity and mechanical properties of composite scaffolds. By

increasing the GO concentration, scaffold stiffness increased to 162 kPa, which was within a suitable range for cardiac tissue engineering applications. Also, Histological assessments of subcutaneously implanted scaffolds at 2 and 4 weeks post implantation in mice exhibited increased cell infiltration within the electroactive scaffolds as well as angiogenic properties of rGO-incorporated constructs due to the presence of rGO. This time, we benefited from the merits of ALG and fabricated scaffolds based on this material which were then coated with different concentrations of GO for cardiac patch utilization. Physicochemical and biological characterizations were performed to find out the optimum concentration of GO for intended application. To the best of our knowledge, this is the first study conducted on ALG containing GO for cardiac application.

## MATERIALS AND METHODS

### Preparation of ALG Scaffolds

The ALG scaffolds were fabricated through freeze drying. For this purpose, 1 wt. % of sodium ALG (Sigma-Aldrich) was dissolved in distilled water. After a complete homogeneous solution, the mixer was cast in Teflon mold and froze at the temperature of -20 °C for 5h and then -80 °C for 12h. After that samples were lyophilized in freeze-dryer device (Alpha 2-4 LDplus, Martin Christ) for 48h at -50 °C. Following that, scaffolds were exposed for 24 hours to a 102 mM CaCl<sub>2</sub> solution made in distilled water as a cross-linker before being thoroughly rinsed to remove any leftover cross-linker and then frozen for another 24 hours.

To coat the scaffolds, different concentrations of aqueous GO (GrapheneX, Kimia Pishtaz) including 0.01, 0.05 and 0.1% (w/v), were prepared. After that, scaffolds were filled with 100 l of each solution, which were then allowed to air dry. The prepared scaffolds were named as was shown in table 1.

### Characterizations

#### Scaffold Characterizations

To investigate the chemical interactions between functional groups of different components in the scaffolds, Fourier transform infrared spectroscopy (FTIR) (PerkinElmer, Frontier) was

**Table 1.** Scaffold preparations and groups Abbreviations

Abbreviations	Scaffolds
ALG	Alginate
ALG-GO-0.01	Alginate+ 0.01% w/v GO
ALG-GO-0.05	Alginate+ 0.05% w/v GO
ALG-GO-0.1	Alginate+ 0.1% w/v GO

utilized in a range of 500–4000 cm<sup>-1</sup>, with a resolution of 1 cm<sup>-1</sup>, at a scan speed of 32 scans/min, in KBr-diluted medium. The test was run on the scaffolds in the presence and absence of the GO coating layer. Scanning electron microscopy (SEM) (Philips, XI30) was used to evaluate the morphology and interconnectivity of pores in the scaffolds. The scaffolds were initially coated with gold via the sputter-coating machine (Bal-Tec, SCD 005) to be ready for SEM imaging. Tensile strength of the scaffolds was determined via a uniaxial testing machine (Model 6027, Instron Company) according to ISO-1798 at room temperature [24]. The test was run on the samples cut into 3×1 cm and fixed in paper frames under a load cell of 5 N, strain rate of 1 mm/min and grip distance of 20 mm. The data including Young's modulus and ultimate tensile strength have been reported as mean ± SD (n=3).

The four-point probe technique (196 system DMM, Keithley) was employed to determine the electrical conductivity of the scaffolds. Each sample was put on the apparatus, and the electric current was measured using the voltage. The electrical conductivity of the scaffolds is calculated and reported by the following formula:  $\sigma = (2.44 \times 10 / S) \times (I/E)$

Where  $\sigma$  is the electrical conductivity, S is the sample side area in m<sup>2</sup>, I is the current through the outer probes in amp, and E is the voltage drop across the inner probe in V. Also, 2.44 is referred to the systematic constant. The data have been reported as mean ± SD, (n=3).

### Cell Culture investigations

This study was approved by the Research Ethics Committee of Tarbiat Modares University under ethics code of IR.MODARES.REC.1399.188.

**Table 2.** Gene sequence of the target and reference gene primers

Species	Gene	Primer	Sequence
Human	VEGFR-2	Forward	5'-CGGTCAACAAAGTCGGGAGA-3'
		Reverse	5'-CAGTGCACCACAAAGACACG-3'
	GAPDH	Forward	5'-CTCATTTCTGCTGATGACA-3'
		Reverse	5'-CTTCCTCCCGTGCTCTTGCT-3'

In-vitro cell culture study was run on the scaffolds according to ISO-10993-5 using HUVECs (Bonyakhteh Stem Cell Bank, Stem cell technology research center: STRC) and L929 s (Royan Stem Cell Bank, Royan Institute) to investigate their cell response in terms of cell proliferation and morphology, respectively [107]. The cells were cultured in Dulbecco's modified Eagle medium F12 (DMEMF12; Invitrogen) containing 10% (v/v) fetal bovine serum (FBS, Gibco) and 1% antibiotic penicillin/streptomycin (Sigma) and passaged when they reach to the density of 90%. The 2<sup>nd</sup> passage was used for this study.

The scaffolds were cut into disks with 5 mm in diameter to be fitted into the bottom of a 96-well microplate (Corning Inc) and each side was sterilized under ultraviolet (UV) radiation for 10 mins. On each sample, 1000000 ( $10^5$ ) cells were seeded, and the samples were incubated at 37 °C in a humidified environment with 5 % CO<sub>2</sub>. A sample containing only cells with medium was considered as the cell culture control.

### In vitro cytocompatibility analysis

The cell viability of the scaffolds was analyzed through MTT (3-(4,5-dimethylthiazol-2-yl)-2,5-diphenyltetrazolium bromide) assay after 48 and

72 hours of incubation. Each time, 100-μL MTT solution (5 mg/mL in PBS) was added to each scaffold being incubated at 37°C and 5% CO<sub>2</sub> for 4 hours. Viable cells with active metabolism convert MTT from yellow into a purple with a maximum light absorbance of about 570 nm due to producing formazan crystals. DMSO was then added into each well to dissolve the formazan crystals. Finally, the absorbed wave length was read at 570 nm via an ELISA microplate reader (IUMS-ER-BP800, Biohit). The data are reported as mean ± SD, (n=3).

### Assessment of Cell Morphology on Scaffolds

SEM was employed to investigate the attachment, spreading, and morphological changes of L929 fibroblasts on the scaffolds after 48 hours of cell culturing. In order to prepare the scaffolds for SEM, they were fixed using 500 μl of glutaraldehyde 2.5% (Sigma-Aldrich) and incubated for 1 hour. Next, the samples were washed with PBS and dehydrated using incremental ethanol including 10%, 30%, 70%, 90% and 100%. Finally, the samples were coated with gold to be ready for SEM imaging.

### RNA Extraction and Quantitative Real-time Polymerase Chain Reaction (qRT-PCR)

Gene expression of VEGFR-2 was investigated for the optimal electroactive scaffold in comparison with the one without coating and the sample-free tissue culture plate after 72 hours of cell culturing through qRT-PCR technique. GAPDH is considered as the housekeeping gene. Briefly, RNA was extracted from the cells using RNeasy mini kit (Qiagen) and its instruction. Quality of the extracted RNA was checked through electrophoresing 2 μl of that on an

**Table 3.** Electrical conductivity of the composite scaffolds

Scaffolds	Electrical conductivity (S.m <sup>-1</sup> )
ALG	$3.78 \pm 0.003(\times 10^{-6})$
ALG/0.01GO	$7.76 \pm 0.001(\times 10^{-6})$
ALG/0.05GO	$8.59 \pm 0.001(\times 10^{-4})$
ALG/0.1GO	$3.45 \pm 0.001(\times 10^{-3})$

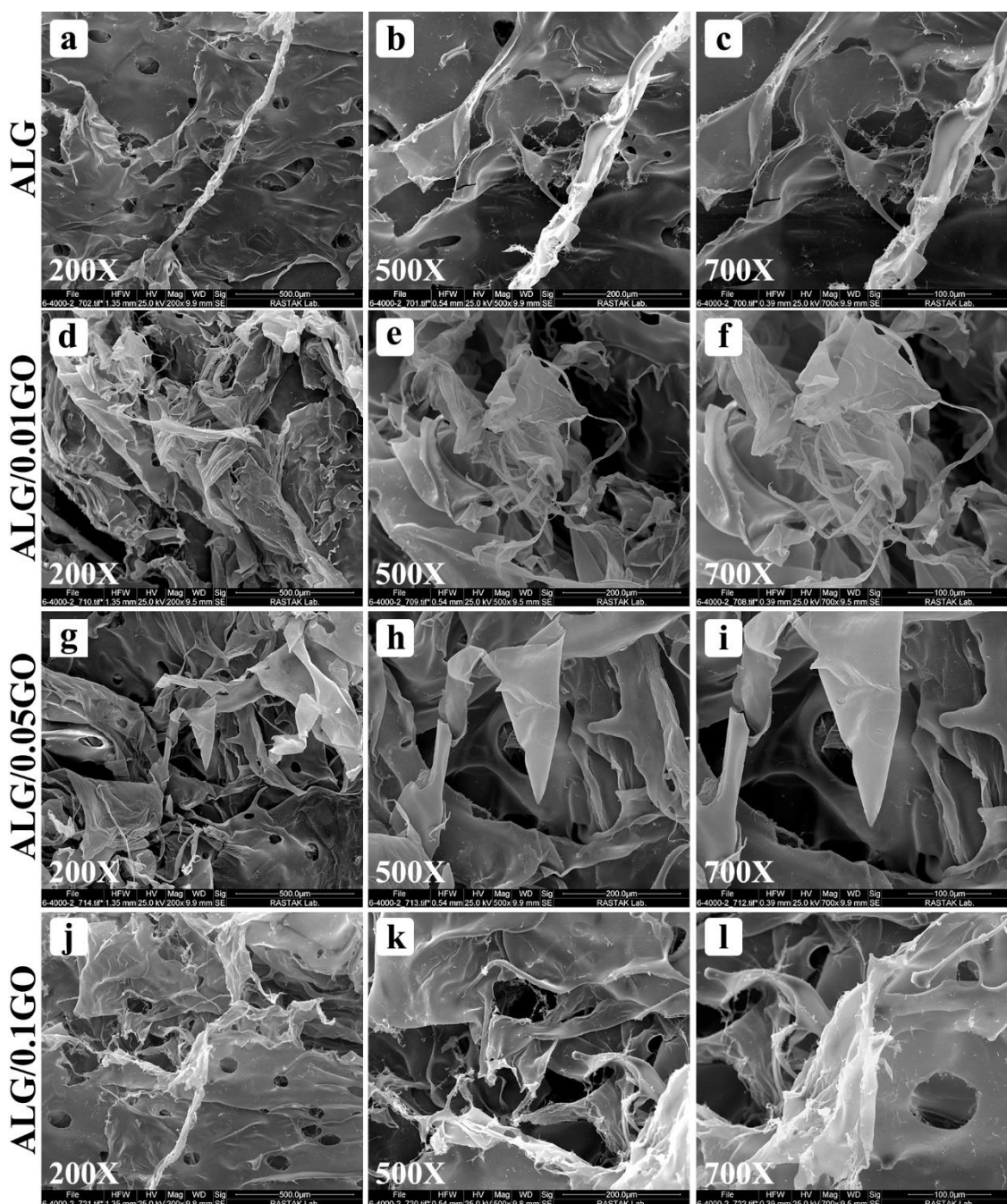


**Figure 1.** SEM images of surface and cross-sections of the prepared hydrogels with different magnification.

agarose gel at the voltage of 140 v for 15 mins. The health of RNA was confirmed regarding visibility of the two major ribosomal RNA (rRNA) bands at 18S and 28S.

The concentration of RNA was quantitated through measuring the optical density (OD) at wavelengths of 230, 260 and 280 nm via a UV-visible Spectrophotometer (NanoDrop ND-1000, Thermo Fisher Scientific Inc).

DNA was removed from the extracted RNA using DNase set kit. The cDNA was synthesized from RNA using RevertAid first strand cDNA synthesis kit (Thermo Fisher Scientific Inc). The gene fragments were amplified through designing a pair of specific gene primers including forward and reverse primers via a DNA sequence analyzer software (gene runner 3.0). The gene sequence related to the target and reference gene primers are presented in Table 2.

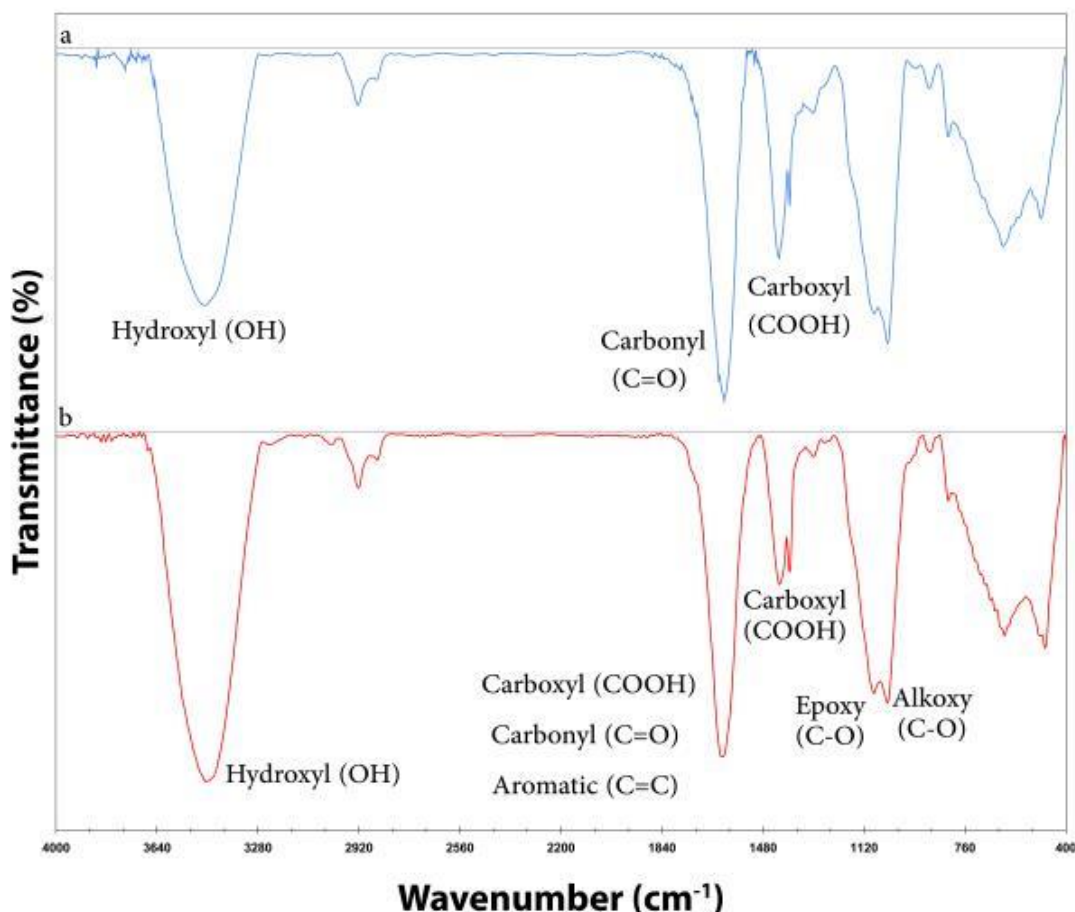


Figure 2. FTIR spectra related to (a) ALG and (b) ALG/0.1GO scaffolds.

Gene expression of the target gene was quantitatively measured using GAPDH as the endogenous control via Maxima SYBR Green/Rox qPCR master mix kit (Thermo Fisher Scientific Inc) according to the following thermal cycle programming. Initial denaturation and denaturation were run at 95°C for 30s (40 cycles) and 5s, respectively. Annealing & extension was run with at 60°C for 20 s. Finally the melting curve was plotted from 95°C up to 60°C with step level of 0.3°C based on the emitted fluorescence against temperature.

#### Statistical analysis

All of the data were statistically analyzed via the statistical software (IBM SPSS statistics version 24 release 24.0.0.0 2016 64-bit edition, SPSS Inc.). One-way analysis of variance (ANOVA) was used for this purpose. A value of  $p \leq 0.05$  was considered as significant difference, while  $p > 0.05$  was considered as insignificant difference. The data obtained from the qRT-PCR was analyzed

using GraphPad Prism (version 8.4.3.686 64-bit edition, Dotmatics Co.).

## RESULTS AND DISCUSSION

### Morphological Assessments

The morphological view of the scaffolds are represented in Fig. 1. The interconnected pores and random orientation and uniform dispersion of GO are observable in all of the scaffolds which can be positively effective on cell behavior of the scaffolds. The interconnected pores have also been reported in other studies conducted on GO ALG composite scaffolds [22]. An increase in the amounts of GO led to a decrease in the size of the pores in all scaffolds which was more obvious in ALG/0.1GO scaffold structure leading to the formation of an almost closed pore.



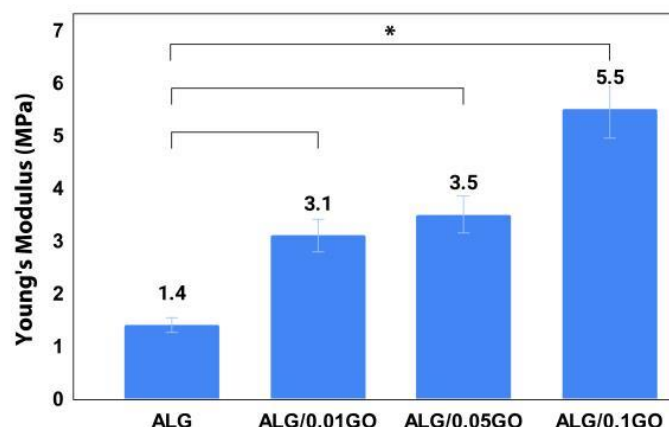


**Figure 3.** Young's modules obtained from the tensile strength test for the scaffolds.

### Chemical Structure

FTIR spectra of the scaffolds in the presence and absence of GO are plotted in Fig. 2. As for ALG spectrum (Fig. 2a), the peaks at  $3467\text{ cm}^{-1}$ ,  $1618\text{ cm}^{-1}$  and  $1422\text{ cm}^{-1}$  are attributed to hydroxyl (OH), carbonyl (C=O) and carboxyl (COOH) functional groups, respectively. As for the spectrum related to the ALG/0.1GO scaffold (Fig. 2b), the absorption peaks at  $3465\text{ cm}^{-1}$ ,  $1624\text{ cm}^{-1}$ ,  $1623\text{ cm}^{-1}$ ,  $1100\text{ cm}^{-1}$  and  $1043\text{ cm}^{-1}$  respectively represent OH, COOH, aromatic

C=C, epoxy and alkoxy of C-O functional groups existed in GO. Moreover, the peaks at  $3467\text{ cm}^{-1}$ ,  $1618\text{ cm}^{-1}$  and  $1422\text{ cm}^{-1}$  are respectively related to hydroxyl, carbonyl and carboxyl groups existed in the sodium alginate. The presence of the GO-related functional groups in the ALG/0.1 scaffold can attest to the presence of both ALG and GO in the composite scaffold. These results are in accordance with other studies[22]

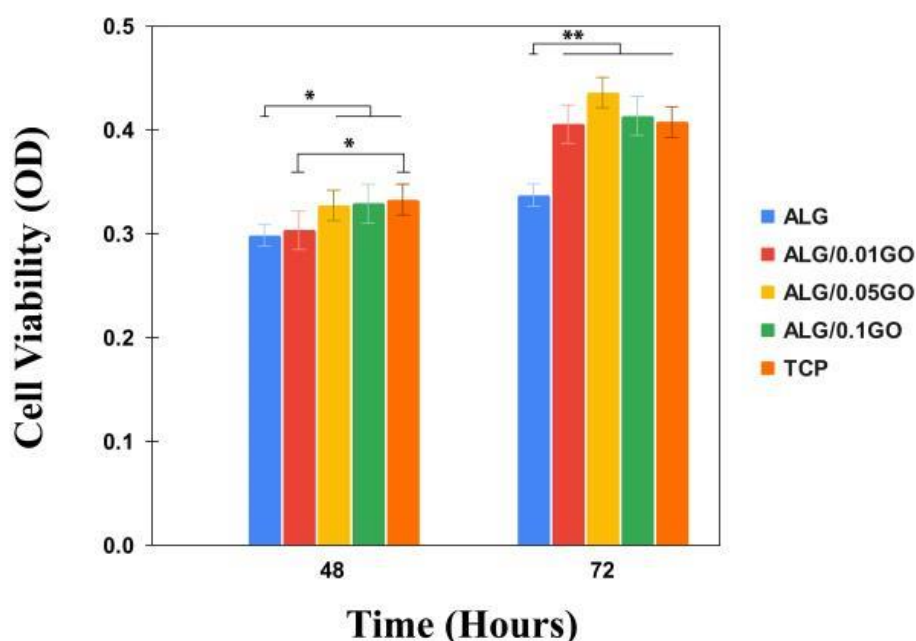


**Figure 4.** Viability of HUVECs cultured on the composite scaffolds evaluated by MTT assay after 48 and 72 hours.

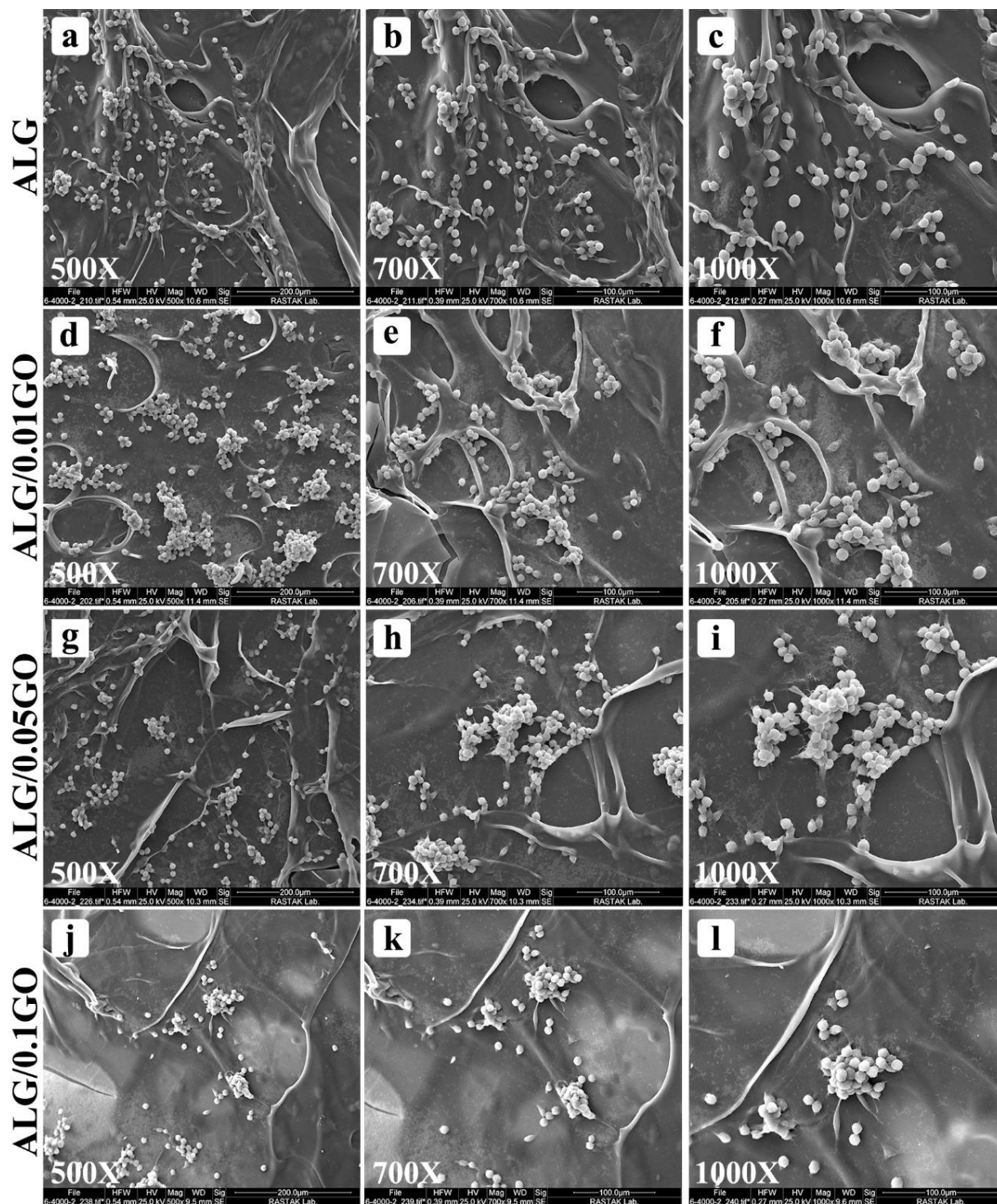


Figure 5. SEM images of L929 fibroblasts morphology cultured on the scaffolds after 48 hours with different magnification.

### Mechanical properties

Young's modulus of the scaffolds obtained from the tensile strength test are presented in Fig. 3. Adding GO from 0.01 wt. % up to 0.1 wt. % significantly increased the Young's modulus from 1.4 MPa for ALG to 5.5 MPa for ALG/0.1GO ( $p \leq 0.001$ ). The obtained results were higher than that was reported by Norahan et al.; a

scaffold composed of Collagen and GO being fabricated by freeze-drying method [15]. Also, the young modulus measured for samples matched the stiffness of heart muscle [4, 19]. The improvement in mechanical qualities was made possible by GO, a bioceramic material with strong intrinsic strength. However, its ceramic origin can increase the scaffold brittleness. A uniform



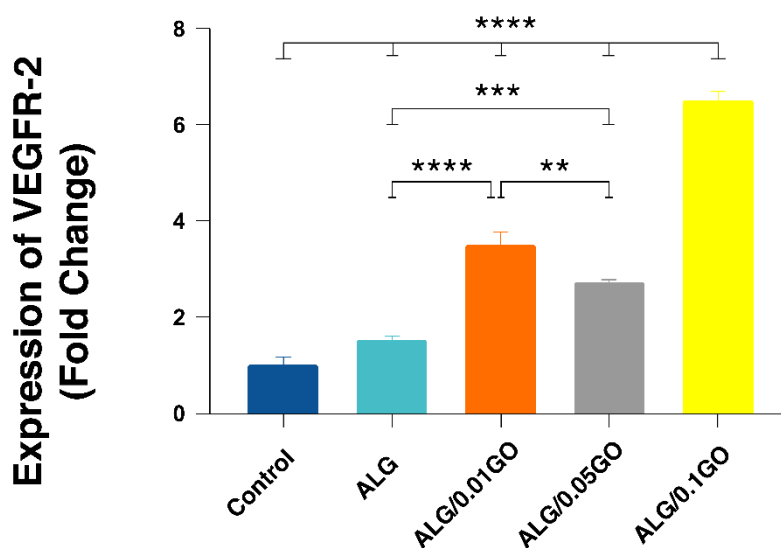


**Figure 6.** Gene expression of VEGFR-2 after 72 hours of HUVECs culturing on the scaffolds. \*\* indicates P value<0.01, \*\*\* indicates P value<0.001 and \*\*\*\* indicates P value<0.0001.

distribution of GO inside the ALG matrix can transform tension from the matrix to the GO particles, leading to a reduction in stress concentration in the polymeric matrix and consequently an enhancement in the tensile strength of the scaffolds [15]. Using GO in ALG hydrogel for cardiac regeneration lead to a desirable increase in the hydrogel toughness [19].

### Electrical Conductivity

The electrical conductivity of the composite scaffolds containing different amounts of GO are tabulated in Table 3. Electrical conductivity is essential for heart tissue engineering scaffolds to induce cardiomyocyte toward an appropriate level of transition in cell signaling and uniform entirely distribution of electrical pulses throughout the cardiac tissue. The presence of GO led to an increase in the electrical conductivity compared to the scaffold without GO. The high intrinsic electrical conductivity of GO let the scaffolds containing GO to be classified in semiconductor group ( $10^{-2}$ - $10^{-6}$  S.m<sup>-1</sup>). The semiconductor scaffolds can electrically be appropriate for cardiac tissue engineering applications [23]. The results of this test are in accordance with previous researches [15]. Also, an electroactive scaffold composed of GO and chitosan which was fabricated by Jiang et al. demonstrated an

optimized electrical conductivity of  $1.6 \times 10^{-3}$  S/m [19].

### Cell Culture Study

#### Cell Viability

The cell viability of HUVECs after 48 and 72 hours of cell culturing on the scaffolds are graphed in Fig. 4 based on MTT assay. According to the data collected after 48 hours, the scaffolds' cell viability improved as GO concentration increased. The scaffolds containing 0.05 wt. % and 0.1 wt. % presented significantly higher cell viability in comparison with the pure ALG scaffold ( $p \leq 0.05$ ). Furthermore after 72 hours of cell culturing, all of the composite scaffolds containing GO, presented significantly enhanced cell viability compared to the ALG scaffold ( $p \leq 0.01$ ). The presence of GO did not have any adverse effect in cell viability of the composite scaffolds, indicating cytocompatibility of GO besides ALG.

#### Morphological Assessments

SEM images to assess the morphology of L929 fibroblasts after 48 hours of cell culturing on the scaffolds are shown in Fig. 5. A higher cell attachment and distribution is obvious for ALG/0.01GO and ALG/0.05GO compared to ALG and ALG/0.1GO. The presence of oxygen-contained functional groups in GO structure and

a desirable roughness on the surface of the composite scaffolds can be an effective factor for cell attachment, distribution and spreading. Moreover, the presence of the open and interconnected pores can provide appropriate places for a better cell nesting. The overconcentration of GO may have filled the holes in the ALG/0.1GO composite scaffold, reducing the number of locations where cells may nest effectively and lowering the cell/scaffold interactions at the scaffold surface.

### Gene Expression

Gene expression of VEGFR-2 related to angiogenesis pathway after 72 hours of cell culturing on the scaffolds regarding GAPDH as the housekeeping gene are shown in Fig. 6 based on qRT-PCR technique. In addition to ALG, the inclusion of GO as an electroactive bioceramic caused the gene expression of VEGFR-2 to considerably increase for the GO-containing scaffolds in comparison to the control sample and pure ALG scaffold ( $p < 0.05$ ). The highest value of gene expression was achieved in the ALG/0.1GO composite scaffold which was significantly higher than all of the other scaffolds and the control sample ( $p \leq 0.05$ ). It is reported that GO coats can stimulate angiogenesis and enhance blood vessels in heart tissue engineering scaffolds. Additionally, GO was added to MSCs, which resulted in the development of cell signaling pathways, a decrease in reactive oxygen species (ROS), modulation of the growth factors VEGF and Akt, and consequently angiogenesis [24].

### CONCLUSION

The ALG scaffolds coated with different concentrations of GO including 0.01, 0.05 and 0.1 wt. % were fabricated through freeze-drying for cardiac tissue engineering applications. Interconnected pores and uniform distribution of GO inside the composite scaffolds structures are important and effective factors in tissue engineering. Presence of ALG and GO functional groups in the FTIR spectra of the scaffolds can confirm formation of composite structure for the scaffolds. Due of the high inherent mechanical strength of GO, an increase in GO concentrations can result in a noticeably increased rise in the

mechanical characteristics of the scaffolds containing GO. An electrical conductivity in range of semiconductors for the scaffolds containing GO make them appropriate for heart tissue engineering scaffolds. The scaffolds containing GO presents a better cell viability of HUVECs compared to the scaffold without GO. GO has no adverse effect on cytocompatibility of the scaffolds. The presence of GO in an optimal concentration lead to an increase in cell attachment due to an optimal level of pore size and interactions at cell/scaffold interfaces. The maximum gene expression of VEGFR-2 was caused by a rise in GO concentration of up to 0.1 weight percent, indicating a desired potential for angiogenesis for this scaffold. The ALG/0.1GO scaffolds may provide a suitable candidate as a cardiac patch for cardiac tissue engineering applications, according to the findings of this study.

### DECLARATIONS

The authors of this manuscript declare no conflicts of interest whatsoever.

### FUNDING

This research was partially supported by Tarbiat Modares University as MSc thesis.

### REFERENCES

1. Mozaffarian D, Benjamin EJ, Go AS, Arnett DK, Blaha MJ, Cushman M, et al. Heart disease and stroke statistics—2015 update: a report from the American Heart Association. *Circ.* 2015; 131(4): e29-e322.
2. Kikuchi K, Poss KD. Cardiac regenerative capacity and mechanisms. *Annu. Rev. Cell Dev. Biol.* 2012; 28: 719.
3. Broughton KM, Sussman MA. Empowering adult stem cells for myocardial regeneration V2.0: success in small steps. *Circ.* 2016; 118(5): 867-880.
4. Bouten CV, Dankers PY, Driessen-Mol A, Pedron S, Brizard AM, Baaijens FP. Substrates for cardiovascular tissue engineering. *Adv. Drug Deliv. Rev.* 2011; 63(4-5): 221-241.
5. Vunjak-Novakovic G, Lui KO, Tandon N, Chien KR. Bioengineering heart muscle: a paradigm for regenerative medicine. *Annu Rev Biomed Eng.* 2011; 13: 245-67.
6. Martinez EC, Kofidis T. Adult stem cells for cardiac tissue engineering. *J. Mol. Cell. Cardiol.* 2010; 50(2): 312-319.

7. Saha K, Keung AJ, Irwin EF, Li Y, Little L, Schaffer DV, Healy KE. Substrate modulus directs neural stem cell behavior. *Biophys J*. 2008; 95(9): 4426-4438.
8. Mathew AP, Uthaman S, Cho KH, Cho CS, Park IK. Injectable hydrogels for delivering biotherapeutic molecules. *Int. J. Biol. Macromol*. 2018 Apr 15; 110:17-29.
9. Garbayo E, Pascual-Gil S, Prosper F, Blanco-Prieto MJ. Bioresorbable polymers for next-generation cardiac scaffolds. In: *Bioresorbable Polymers for Biomedical Applications: From Fundamentals to Translational Medicine*. 2017; p. 445-467.
10. Martins AM, Eng G, Caridade SG, Mano JF, Reis RL, Vunjak-Novakovic G. Electrically conductive chitosan/carbon scaffolds for cardiac tissue engineering. *Biomacromolecules*. 2014; 15(2): 635-643.
11. Zia KM, Tabasum S, Nasif M, Sultan N, Aslam N, Noreen A, Zuber M. A review on synthesis, properties and applications of natural polymer based carrageenan blends and composites. *Int. J. Biol. Macromol*. 2017 Mar; 96: 282-301.
12. Saghebasl S, Akbarzadeh A, Gorabi AM, Nikzamir N, SeyedSadjadi M, Mostafavi E. Biodegradable functional macromolecules as promising scaffolds for cardiac tissue engineering. *Polymers for Advanced Technologies*. 2022.
13. Laflamme MA, Murry CE. Heart regeneration. *Nature*. 2011; 473(7347): 326-335.
14. Lee LC, Wall ST, Klepach D, Ge L, Zhang Z, Lee RJ, Hinson A, Gorman JH 3rd, Gorman RC, Guccione JM. Algisyl-LVR™ with coronary artery bypass grafting reduces left ventricular wall stress and improves function in the failing human heart. *Int. J. Cardiol*. 2013 Oct 3; 168(3): 2022-8.
15. Norahan MH, Amroon M, Ghahremanzadeh R, Mahmoodi M, Baheiraei N. Electroactive graphene oxide-incorporated collagen assisting vascularization for cardiac tissue engineering. *J. Biomed. Mater. Res. A*. 2019 Jan; 107(1): 204-219.
16. Venugopal JR, Prabhakaran MP, Mukherjee S, Ravichandran R, Dan K, Ramakrishna S. Biomaterial strategies for alleviation of myocardial infarction. *J. R. Soc. Interface*. 2012; 9(66): 1-19.
17. Mousavi A, Vahdat S, Baheiraei N, Razavi M, Norahan MH, Baharvand H. Multifunctional conductive biomaterials as promising platforms for cardiac tissue engineering. *ACS. Biomater. Sci. Eng*. 2021 Jan 11; 7(1): 55-82.
18. Lee TJ, Park S, Bhang SH, Yoon JK, Jo I, Jeong GJ, Hong BH, Kim BS. Graphene enhances the cardiomyogenic differentiation of human embryonic stem cells. *Biochem. Biophys. Res. Commun*. 2014 Sep 12; 452(1): 174-80.
19. Jiang L, Chen D, Wang Z, Zhang Z, Xia Y, Xue H, Liu Y. Preparation of an electrically conductive graphene oxide/chitosan scaffold for cardiac tissue engineering. *Appl. Biochem. Biotechnol*. 2019 Aug; 188(4): 952-964.
20. Choe G, Kim SW, Park J, Park J, Kim S, Kim YS, Ahn Y, Jung DW, Williams DR, Lee JY. Anti-oxidant activity reinforced reduced graphene oxide/alginate microgels: mesenchymal stem cell encapsulation and regeneration of infarcted hearts. *Biomaterials*. 2019 Dec; 225: 119513.
21. ISO 1798:2008. Flexible cellular polymeric materials—Determination of tensile strength and elongation at break. International Organization for Standardization.
22. Wan Y, Chen X, Xiong G, Guo R, Luo H. Synthesis and characterization of three-dimensional porous graphene oxide/sodium alginate scaffolds with enhanced mechanical properties. *Mater. Express*. 2014 Sep; 4(5): 429-434.
23. Chaudhuri B, Bhadra D, Moroni L, Pramanik K. Myoblast differentiation of human mesenchymal stem cells on graphene oxide and electrospun graphene oxide-polymer composite fibrous meshes: importance of graphene oxide conductivity and dielectric constant on their biocompatibility. *Biofabrication*. 2015 Feb; 7(1): 015009.
24. Mukherjee S, Sriram P, Barui AK, Nethi SK, Veeriah V, Chatterjee S, Suresh KI, Patra CR. Graphene Oxides Show Angiogenic Properties. *Adv. Healthc. Mater*. 2015 Aug; 4(11): 1722-1732.